AMERICAN SOCIETY FOR MICROBIOLOGY | mBio®

RESEARCH ARTICLE

Early Interactions of Murine Macrophages with *Francisella tularensis* Map to Mouse Chromosome 19

Avner Fink,[a] Musa A. Hassan,[b,c] Nihal A. Okan,[a] Michal Sheffer,[d] Ana Camejo,[b] Jeroen P. J. Saeij,[b,e] Dennis L. Kasper[a]

Department of Microbiology and Immunobiology, Harvard Medical School, Boston, Massachusetts, USA[a]; Department of Biology, Massachusetts Institute of Technology, Cambridge, Massachusetts, USA[b]; Wellcome Trust Centre for Molecular Parasitology, University of Glasgow, Glasgow, United Kingdom[c]; Dana-Farber Cancer Institute, Harvard Medical School, Boston, Massachusetts, USA[d]; Department of Pathology, Microbiology & Immunology, University of California, Davis, Davis, California, USA[e]

ABSTRACT **Differences among individuals in susceptibility to infectious diseases can be modulated by host genetics. Much of the research in this field has aimed to identify loci within the host genome that are associated with these differences. In mice, A/J (AJ) and C57BL/6J (B6) mice show differential susceptibilities to various pathogens, including the intracellular pathogen *Francisella tularensis*. Because macrophages are the main initial target during *F. tularensis* infection, we explored early interactions of macrophages from these two mouse strains with *F. tularensis* as well as the genetic factors underlying these interactions. Our results indicate that bacterial interactions with bone marrow-derived macrophages (BMDMs) during early stages of infection are different in the AJ and B6 strains. During these early stages, bacteria are more numerous in B6 than in AJ macrophages and display differences in trafficking and early transcriptional response within these macrophages. To determine the genetic basis for these differences, we infected BMDMs isolated from recombinant inbred (RI) mice derived from reciprocal crosses between AJ and B6, and we followed early bacterial counts within these macrophages. Quantitative trait locus (QTL) analysis revealed a locus on chromosome 19 that is associated with early differences in bacterial counts in AJ versus B6 macrophages. QTL analysis of published data that measured the differential susceptibilities of the same RI mice to an *in vivo* challenge with *F. tularensis* confirmed the *F. tularensis* susceptibility QTL on chromosome 19. Overall, our results show that early interactions of macrophages with *F. tularensis* are dependent on the macrophage genetic background.**

IMPORTANCE ***Francisella tularensis* is a highly pathogenic bacterium with a very low infectious dose in humans. Some mechanisms of bacterial virulence have been elucidated, but the host genetic factors that contribute to host resistance or susceptibility are largely unknown. In this work, we have undertaken a genetic approach to assess what these factors are in mice. Analyzing early interactions of macrophages with the bacteria as well as data on overall susceptibility to infection revealed a locus on chromosome 19 that is associated with both phenotypes. In addition, our work revealed differences in the early macrophage response between macrophages with different genetic backgrounds. Overall, this work suggests some intriguing links between *in vitro* and *in vivo* infection models and should aid in further elucidating the genetic circuits behind the host response to *Francisella tularensis* infection.**

Received 29 December 2015 **Accepted** 6 January 2016 **Published** 15 March 2016

Citation Fink A, Hassan MA, Okan NA, Sheffer M, Camejo A, Saeij JPJ, Kasper DL. 2016. Early interactions of murine macrophages with *Francisella tularensis* map to mouse chromosome 19. mBio 7(2):e02243-15. doi:10.1128/mBio.02243-15.

Editor Andrew B. Onderdonk, Brigham and Women's Hospital

Address correspondence to Dennis L. Kasper, dennis_kasper@hms.harvard.edu.

This article is a direct contribution from a Fellow of the American Academy of Microbiology. External solicited reviewers: Eric J. Rubin, Harvard School of Public Health; Timothy J. Sellati, Southern Research Institute.

Francisella tularensis is a highly pathogenic, facultative intracellular Gram-negative bacterium that infects a broad range of hosts, including humans. In humans, even a very low dose of this bacterium can cause tularemia, a severe and potentially lethal disease. *F. tularensis* can infect hosts through various routes, with the intranasal route causing the most severe disease. Laboratory mice have been extensively used as a model in which to explore various aspects of this disease, including immunological response, bacterial life cycle within the host, and vaccine development (1–4). To date, the fully virulent SchuS4 strain and the attenuated live vaccine strain (LVS) of *F. tularensis* have been the most commonly used mouse models of infection.

Although different mouse strains exhibit various susceptibilities to *F. tularensis* infection (5, 6), the genetic basis for this difference remains poorly understood. A locus on chromosome 1, designated Bcg, has been associated with differences in susceptibility to *F. tularensis* (7). This locus harbors the *Slc11a1* gene coding for natural-resistance-associated macrophage protein 1 (NRAMP1), a divalent metal ion transporter. In mice, two different alleles have been described for this gene that control sensitivity to *Salmonella enterica* serovar Typhimurium, *Mycobacterium bovis*, and *Leishmania donovani* (reviewed in reference 8) as well as to *Francisella* infection (7). In *Francisella*, natural variation within this gene affects the mi-

croenvironment of the phagosome and changes the ability of *F. tularensis* to reside within the phagosome (9). Despite these intriguing early reports, there have been no further studies on the connection of this gene to *F. tularensis* resistance.

Tumor necrosis factor alpha (TNF-α) and gamma interferon (IFN-γ) are major cytokines involved in controlling tularemia *in vivo* (2, 10, 11). Other genes, including those encoding Toll-like receptor 2 (TLR2), AIM2, and cGAS (12–14), have been shown to control tularemia. AIM2 and cGAS are important intracellular sensors for *Francisella* DNA, whereas TLR2 detects lipopeptides on the bacterial surface (15, 16). Recent studies have shown that the bacteria can escape immune clearance in dendritic cells and macrophages by actively suppressing the immune response in these cells (17, 18). Together, the accumulating data suggest an intricate relationship between the bacteria and host defense mechanisms.

Macrophages are considered the primary target site for *Francisella* infection and replication (19, 20). A recent study examining the early interactions of *F. tularensis* with various cells after intranasal challenge revealed that the majority of the bacteria were associated with alveolar macrophages at the initiation of infection (3). The life cycle of *F. tularensis* within macrophages involves entry into the cells via opsonization-dependent or -independent pathways. Opsonized bacteria interact with different receptors, such as the C3 complement receptor (CR3), Fc receptor γ, or scavenger receptor A (21, 22). Unopsonized bacteria enter the cells via interaction with the mannose receptor (23, 24). After internalization into the host cell, *Francisella* is trafficked through the early and late phagosome but prevents fusion of the phagosome with the lysosome and escapes into the cytosol, where it replicates to high numbers before lysing the cell to initiate a new round of infection (25). Whether natural genetic variation within the host modulates any of these processes and thereby affects disease progression is unknown.

Two major strains of laboratory mice, A/J (AJ) and C57BL/6J (B6), differ significantly in susceptibility to experimental tularemia (6). In this study, we used AXB/BXA recombinant inbred (RI) mice and their progenitors (AJ and B6 mice) to investigate the relationship between macrophage genotype and response to *F. tularensis*. AXB/BXA mice are derived from an initial reciprocal cross of AJ (A) and C57BL/6J (B) mice followed by multiple ($\geq$20) rounds of inbreeding resulting in a homozygous and stable mosaic of blocks of the parental alleles in their genomes (26). When challenged with *F. tularensis*, these mice showed a continuous phenotype, which is typical of a complex trait (5). Although the phenotype of these mice in response to *F. tularensis* infection was described, the genetic basis underlying this differential susceptibility was not discussed. RI mice were recently used to explore the genetic factors that control the variable macrophage response to stimulation with IFN-γ plus TNF-α and the various susceptibilities of macrophages to infection with the intracellular pathogen *Toxoplasma gondii* (27).

Focusing on early bacterial association with macrophages and using macrophages from RI mice, we have identified the specific loci that are linked with differences in the early interactions of *F. tularensis* with murine macrophages. Moreover, quantitative trait locus (QTL) analysis of the published *in vivo* data suggests that the same locus affecting early macrophage-*F. tularensis* interactions is associated with differential susceptibilities to *in vivo* infection as well.

RESULTS

Differences in susceptibility to *F. tularensis* infection *in vivo* are dependent on host genetic background and are associated with differences in dissemination. AJ and B6 mice have significantly different bacterial burdens in the spleen at day 5 after *F. tularensis* infection (5). In addition, mice from an RI library derived from these strains display a continuous phenotype in response to *F. tularensis* challenge (5). Initially, we confirmed major survival differences between the AJ (sensitive) and B6 (resistant) mouse strains after intranasal challenge with *F. tularensis* LVS (Fig. 1A). The median times to death after intranasal challenge with 250 CFU were 8 and 12 days for AJ and B6 mice, respectively ($P = 0.002$ [log rank test]). In addition to survival, we assessed bacterial burden in several major organs. Bacterial burdens in the lung on day 6 after infection did not differ significantly in the two mouse strains (Fig. 1B); this result suggested similar abilities of *F. tularensis* to colonize the lungs—the initial site for colonization—in the two strains. In contrast, bacterial numbers in the spleen and liver differed significantly in AJ and B6 mice. In both cases, bacterial counts on day 6 after infection were significantly lower in B6 mice than in AJ animals (Fig. 1C and D). Taken together, these results confirm the differences in susceptibility between these strains in terms of both survival and bacterial burden in major organs.

Differences in bacterial counts during *in vitro* infection are manifested mainly at early time points. As macrophages are the main initial target in *F. tularensis* infection, we tested whether the *in vivo* differences in susceptibility between AJ and B6 mice are also evident during *in vitro* infection in macrophages. For this purpose, we used a well-established, synchronized model of infection, strictly measuring only intracellular bacteria (for details, see reference 28 and Materials and Methods). Testing bone marrow-derived macrophages (BMDMs), we found that the bacterial growth index (the ratio between bacterial counts at 24 h and 2 h) was significantly higher for AJ than for B6 BMDMs (Fig. 2A). The differences in bacterial counts were evident at the initial stage of infection (2 h after infection) (Fig. 2B), whereas at the later time point (24 h) there was no significant difference between bacterial counts in BMDMs from the two sources (Fig. 2C). The similar levels of expression of major macrophage markers such as CD11b and F4/80 in BMDMs from these two mouse strains suggested similar maturation states (Fig. 2D).

To assess the relevance of these results to infection with a fully virulent strain, we tested *F. tularensis* SchuS4 bacterial proliferation in these BMDMs. Similarly to the LVS, SchuS4 had a higher bacterial growth index in AJ macrophages than in B6 cells, with significantly different bacterial counts at 2 h but not at 24 h after infection (see Fig. S1 in the supplemental material). Finally, in an *ex vivo* experiment, a similar trend was observed in resting unstimulated peritoneal macrophages (results not shown). Overall, these data indicate that *F. tularensis* is initially better at entering B6 macrophages but, once inside the cells, grows better in AJ macrophages.

Differences in bacterial growth are dependent on early bacterium-macrophage interactions and on the macrophage activation state. The differences between the 2 cell lines 2 h after *F. tularensis* infection prompted us to ask whether there is a difference in bacterial uptake. Confocal microscopy of BMDMs at the initiation of *F. tularensis* infection revealed greater bacterial asso-

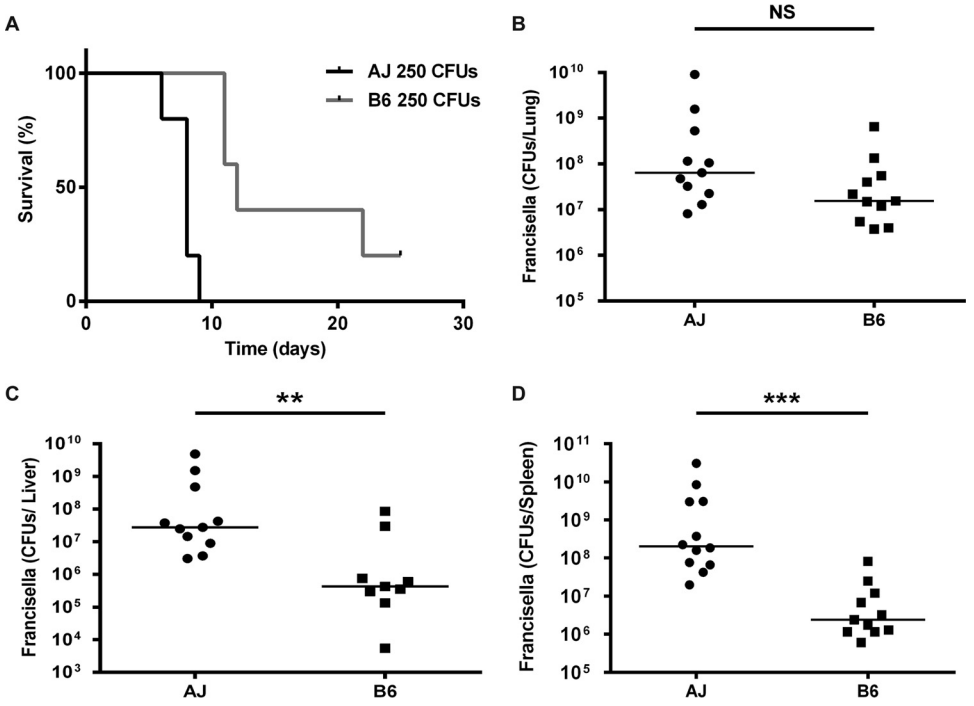

FIG 1 Differential susceptibilities of AJ and B6 mice to *F. tularensis* LVS infection. (A) Mice ($n = 5$) of either the AJ or the B6 strain were infected intranasally with LVS (250 CFU), and mortality in response to infection was followed for up to 25 days. Both time to death and percent mortality differed in the two strains. (B to D) AJ or B6 mice were infected intranasally with 250 bacterial CFU. Bacterial counts in lungs (B), liver (C), and spleen (D) were evaluated on day 6 after infection. While no statistically significant difference was found at the primary site of infection (lungs, $P = 0.075$), differences were statistically significant in liver ($P = 0.0167$) and spleen ($P < 0.001$). Statistical analysis was done with the Mann-Whitney nonparametric test. NS, not significant.

ciation with B6 than with AJ BMDMs as well as significant differences in the percentages of cells infected (Fig. 3A and B). These results are in line with our observations at 2 h after infection and suggest that, at early time points during infection, bacterial numbers are higher in B6 than in AJ macrophages. Comparison of these data with those on the uptake of *S. enterica* serovar Typhimurium by these macrophages suggested no significant difference in the percentages of macrophages infected with *S. enterica* as well as no difference in bacterial counts per cell (Fig. 3C and D).

Macrophage activation by various pathways can strongly influence the macrophage phenotype. We tested whether the macrophage activation state affects the differences observed in bacterial uptake or growth. Activation of the cells with lipopolysaccharide (LPS) from *Escherichia coli* prior to infection abolished the differential bacterial growth indices of the strains (see Fig. S2 in the supplemental material). LPS treatment resulted in higher bacterial counts at both early and late time points, with similar magnitudes for the two cell lines. Thus, LPS activation resulted in similar levels of bacterial growth in the two BMDM strains.

Insights into the specific pathways that modulate differential susceptibilities to *F. tularensis* in AJ and B6 BMDMs. We assessed whether the observed differences in bacterial counts are associated with different transcriptional responses in B6 and AJ BMDMs. As we were interested in early time points, we infected these 2 cell lines with *F. tularensis in vitro* and used RNA sequencing (RNA-seq) to profile their transcriptional responses in the resting state and at 2, 4, and 10 h after infection. We further analyzed our data with gene-set enrichment analysis (GSEA) to obtain a detailed profile of the specific pathways that are either suppressed or induced during early infection in macrophages. Based on an analysis of more than 900 cellular pathways and networks, our results suggest that the overall responses of the 2 cell lines are highly similar (Fig. 4A). The response consists mainly of a strong nuclear factor κB (NFκB) response 2 h after infection that turns into an interferon response at 10 h. At the latter time point, IFN type I and type II pathways are significantly upregulated (Table 1). Although the overall profiles are highly similar, a closer look at the exact genes that are upregulated within these pathways reveals significant differences between the strains. Overall, at 2 h after infection, expression of many proinflammatory genes (such as those encoding TNF, CXCL1, CXCL2, and interleukin-1β [IL-1β]) is induced to a higher degree in B6 than in AJ macrophages. The picture is similar for various genes that constitute the interferon response (e.g., those encoding interferon regulatory factor 1 [IRF1], IFIT1 to IFIT3, ISG15, and MX1), which are significantly more upregulated in B6 than in AJ macrophages (Fig. 4B and C). Furthermore, compared to those in uninfected cells (i.e., at time zero), TNF gene transcript levels at 4 h and 10 h after infection seem to remain high for B6 but not for AJ. The exact downstream effects of these differential responses remain unknown, as the levels of primary proinflammatory cytokines such as TNF-α, interleukin 6 (IL-6), IL-1β, and IFN-γ are very low in the supernatants of both cell lines, even after 24 h (results not shown).

In addition, we investigated the early trafficking of the bacteria within the macrophages. Early trafficking and movement into the cytosol can have a significant effect on the intracellular fate of bacteria and thus on the infection process (29). We looked at bacterial colocalization with the early endosomal marker EEA1 at

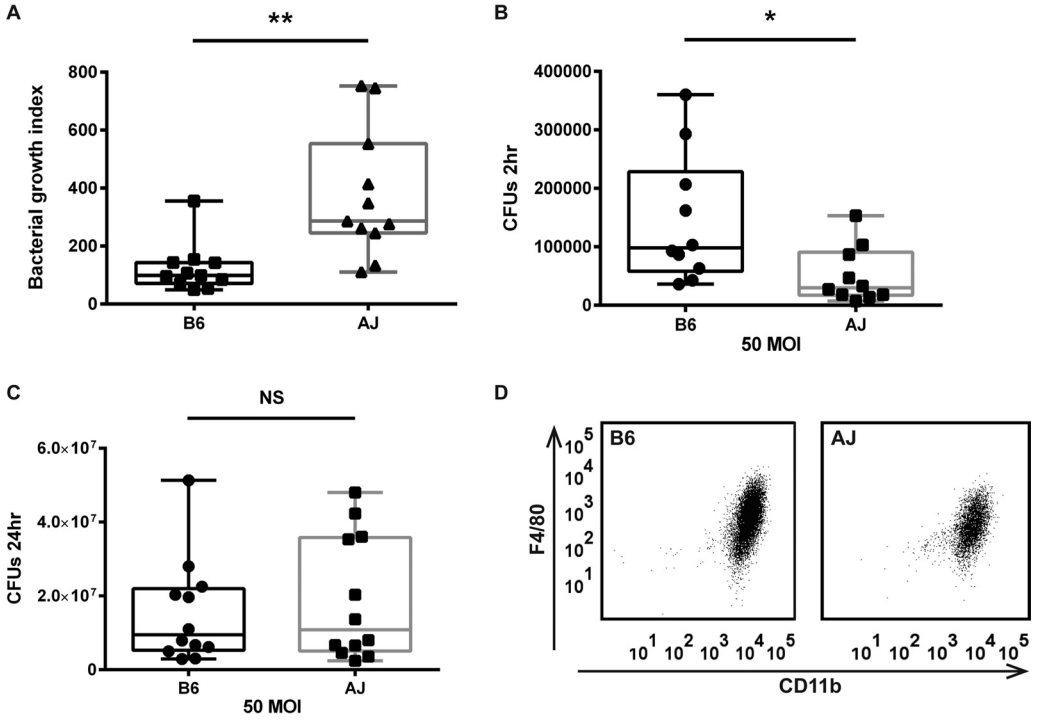

FIG 2 Differential growth of *F. tularensis* LVS in AJ and B6 BMDMs. (A) Bacterial growth was assessed in an *in vitro* infection assay. Intracellular bacterial counts were measured 2 h and 24 h after infection at an MOI of 50. The bacterial growth index represents the ratio between bacterial counts at 24 h and 2 h (CFU at 24 h/CFU at 2 h; $P = 0.002$). (B) Initial intracellular bacterial counts 2 h after infection ($P = 0.023$). (C) Final intracellular bacterial counts 24 h after infection ($P = 0.57$). Each data point represents the average of results from a single experiment; statistical analysis was done with the unpaired *t* test. (D) FACS analysis of AJ and B6 BMDMs. BMDMs (day 8) were stained for major macrophage markers CD11c and F4/80. The overall staining patterns were similar for the 2 cell populations.

the initiation of infection and after 1 h and at colocalization with the LAMP1 late endosomal marker after 2 h (see Fig. S3 in the supplemental material). While there was no significant difference in the percentages of bacteria colocalized with EEA1, after 2 h a larger percentage of bacteria were associated with LAMP1 in B6 than in AJ macrophages. Taken together, our results suggest differential trafficking of bacteria in these two lines (Fig. 4D and E).

Finally, we investigated whether there are differences in cytotoxicity between these 2 cell lines in response to *F. tularensis* infection. Cytotoxicity in response to *Francisella* infection is dependent on AIM2 inflammasome activation (30). In the resting state, both cell lines exhibited very low cytotoxicity; at a high multiplicity of infection (MOI), some cytotoxicity was observed, but its levels were not different in the two strains (Fig. 4F).

***In vitro F. tularensis* infection of BMDMs derived from RI mice.** Once we implemented an *in vitro* infection system that showed differences in bacterial numbers within macrophages from B6 and AJ mice at early time points, we monitored bacterial counts 2 h after infection of BMDMs from 26 RI mice with *F. tularensis* at an MOI of 50. Our results showed a gradual phenotype across the library that is typical for a complex multi-trait phenotype (Fig. 5). While BMDMs derived from AJ mice had the fewest bacteria per cell, B6 macrophages exhibited an intermediate phenotype in which several other RI strains had higher numbers of bacteria.

QTL analysis reveals a locus on chromosome 19 that is associated with bacterial numbers at early time points after infection. The differences in *F. tularensis* association with macrophages at the initiation of infection as well as the differences in early trafficking and early transcriptional response prompted us to explore the genetic loci associated with these phenotypes. As all these phenotypes represent changes occurring early in infection, we performed QTL analysis of bacterial numbers in RI BMDMs 2 h after infection. Our analysis suggested that bacterial counts at 2 h corresponded to a locus on chromosome 19 (22.410 Mb; Fig. 6A).

Previous studies showed that bacterial numbers measured on day 5 after infection in the spleen of mice from the RI library show a typical gradual phenotype (5). To gain insight into the genetic loci behind this phenotype, we performed QTL analysis on this data set. Our analysis suggested three different loci that are associated with the *in vivo* phenotype located on chromosomes 1 (79.900 Mb), 2 (27.662 Mb), and 19 (21.572 Mb), respectively (Fig. 6B). To test whether the *in vivo* loci interact with one another, we fixed the genotypes in a specific locus and measured the effect on the other loci. A significant increase in the logarithm-of-odds (LOD) score for a specific QTL suggests that it interacts with the QTL that is fixed. We showed that the QTLs on chromosomes 1 and 2 interact with each other, while the QTL on chromosome 19 was not affected (Fig. 6C, D, and E).

DISCUSSION

Susceptibility to bacterial infection is often a complex trait. Thus, the interaction of multiple genes is likely to determine the outcome of infection (for a review, see reference 31). Just like individuals within a community, different inbred mouse strains show different levels of susceptibility to various pathogens (5, 26, 32).

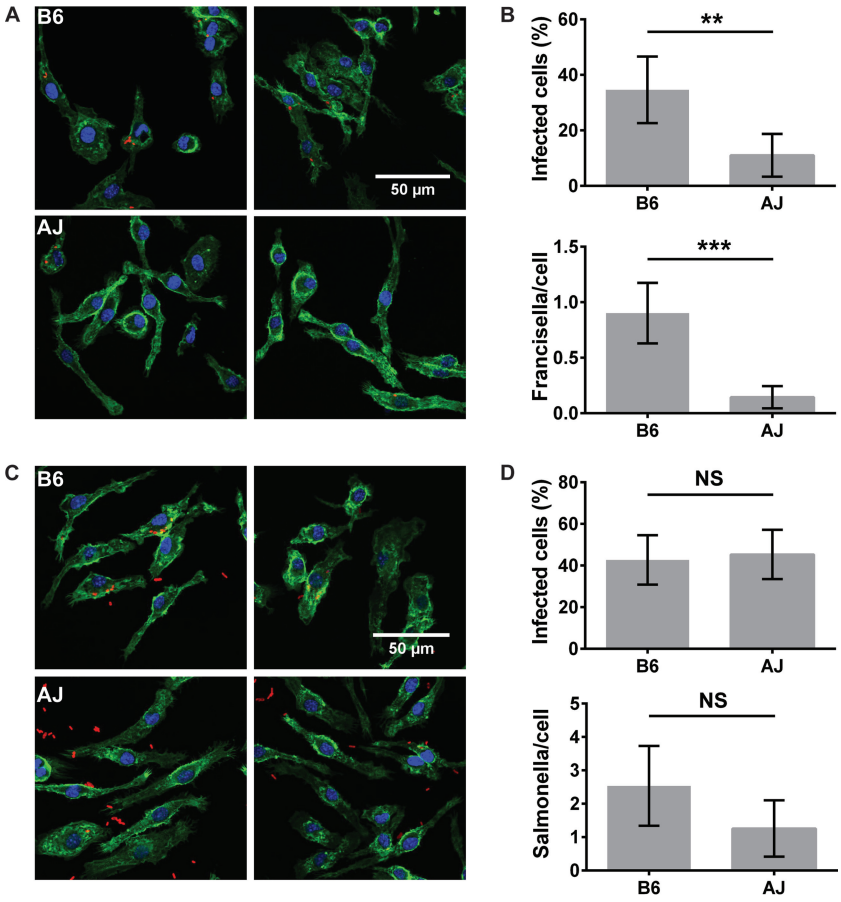

FIG 3 Differences in *F. tularensis* LVS association with AJ and B6 BMDMs at the initiation of infection. (A) Bacteria were added to BMDMs and spun down to allow a synchronized starting point for infection. Immediately after the spin, cells with bacteria were fixed with paraformaldehyde. BMDMs were stained with actin phalloidin (green); nuclei were stained with DAPI (blue); and bacteria were stained with antibodies to LPS (red). Images are from a representative experiment. (B) Average bacterial counts per cell and percentages of cells infected were found to be markedly lower for AJ than for B6 macrophages. Analysis was done on 150 to 250 cells per experiment. (C and D) BMDMs were infected with *S.* Typhimurium (SL1344) in a manner similar to that described for panels A and B. Neither bacterial counts per cell ($P = 0.067$) nor percentages of macrophages infected ($P = 0.72$) differed significantly between the two strains. For both *F. tularensis* and *S.* Typhimurium, the results shown represent three independent experiments. Statistical analysis was done with single-factor analysis of variance (ANOVA).

Although early work identified differences in susceptibility to *F. tularensis* infection among several commonly used mouse strains, the genetic variation underlying these differences remains unknown.

Previous studies showed that AJ and B6 mice differ in susceptibility to *in vivo* infection with *F. tularensis*. Because of the complexity of *in vivo* challenge and the multitude of possible biochemical networks and molecular interactions that may influence disease outcome, we decided to explore this area using a simplified and systematic approach: *in vitro* infection of BMDMs with *F. tularensis*. We hypothesized that because macrophages are a primary target for *F. tularensis* infection, especially in its early stages (3), differences in susceptibility to *in vivo* infection in different mouse strains might be recapitulated *in vitro*. Hence, we further hypothesized that a more confined *in vitro* challenge would be more useful to define the underlying genetics.

Our results clearly show differences in *F. tularensis* LVS growth within these macrophages. Bacterial growth is faster in AJ (susceptible strain) than in B6 (resistant strain) macrophages. Results were similar for fully virulent strain SchuS4. This difference in growth reflects differences between bacterial counts in the 2 cell lines at early time points. Abolishing the differences in early stages of infection by activating cells with LPS before adding *F. tularensis* resulted in similar levels of bacterial growth in the 2 cell lines. This result suggests that the initial resting state of the macrophages is a crucial factor in studies of these differences and is of broader significance in experiments performed with prestimulated macrophages (e.g., thioglycolate-elicited peritoneal macrophages). In these cases, results should preferably be confirmed by complementary experiments performed with resting unstimulated macrophages.

In addition to differences in bacterial growth and counts at early time points during infection, our results show differences between B6 and AJ macrophages in bacterial uptake (i.e., early association) and trafficking as well as in transcriptional response during *in vitro* infection. Using QTL analysis of early bacterial counts within macrophages from a library of RI mice harboring mosaic genomes of AJ and B6, we defined a QTL on chromosome 19 that is associated with this phenotype. Furthermore, analysis of available data on *in vivo* infection revealed a QTL on chromosome

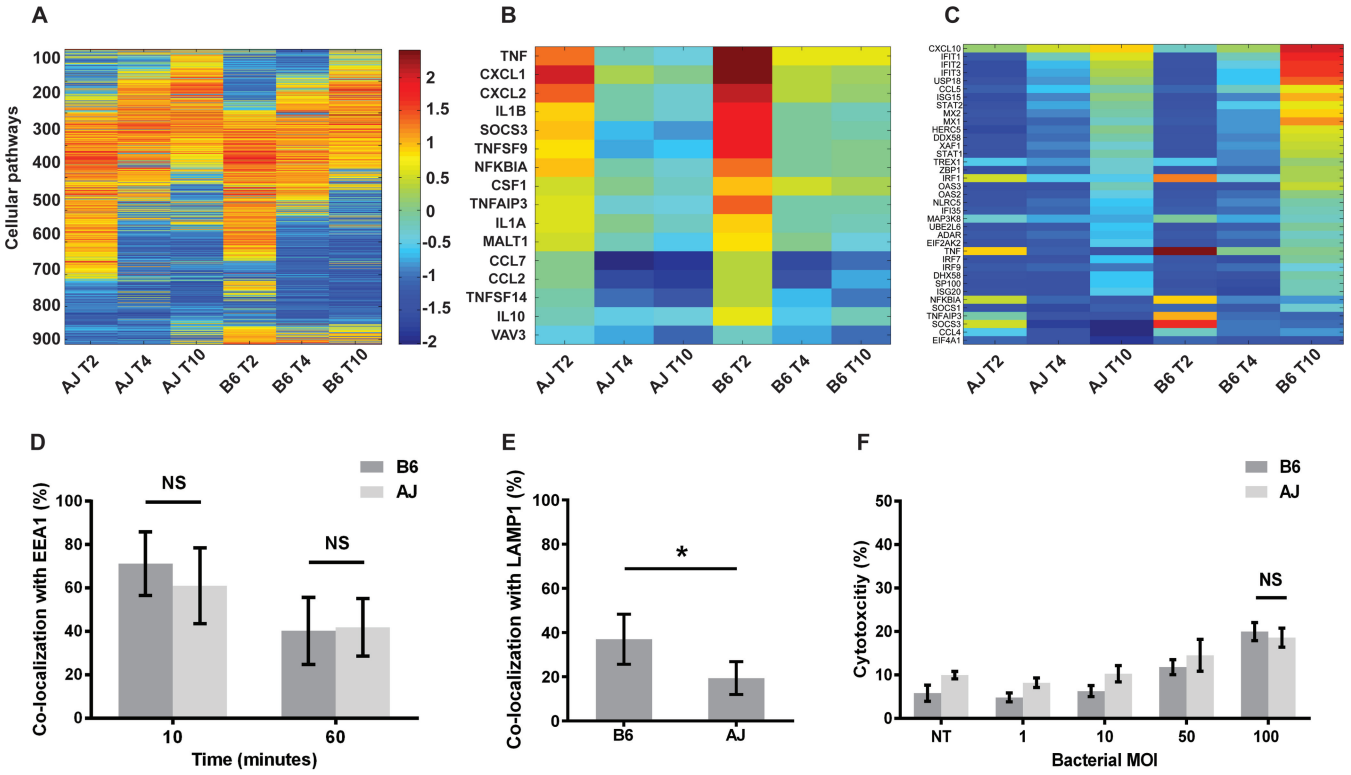

FIG 4 Analysis of differences between AJ and B6 BMDMs in transcriptional response, bacterial trafficking, and cytotoxicity throughout infection with *F. tularensis* LVS. (A) BMDMs were infected, and early macrophage transcriptional response was monitored. RNA-seq data from 2, 4, and 10 h after infection were analyzed on a GSEA platform. More than 900 pathways were scored for upregulation (red) or downregulation (blue) in comparison to resting, untreated BMDMs. The overall transcriptional responses to *in vitro* infection were remarkably similar for the 2 cell lines. (B and C) Selected genes from the top 10 most upregulated immune-related pathways at 2 h (B) and 10 h (C). Shown are all genes whose expression levels were at least 1.5-fold different between AJ and B6 BMDMs. (D and E) After BMDM infection, LVS colocalization with the early endosomal marker EEA1 was assessed at 10 and 60 min (D) and colocalization with the late endosomal marker LAMP1 was assessed at 2 h (E). While no difference was observed for EEA1, a significant difference was documented for LAMP1, with more colocalization in the B6 strain than in the AJ strain. The results shown represent three independent experiments, with 100 to 200 cells analyzed at each time point. (F) BMDM cytotoxicity in response to LVS infection was assessed 24 h after infection. Levels of cytotoxicity did not differ significantly between AJ and B6 BMDMs. Statistical analysis was done with one-way ANOVA ($P = 0.39$).

19 that overlaps the *in vitro* QTL as well as two other QTLs on chromosomes 1 and 2.

The finding of a QTL on chromosome 1 that is associated with differential levels of susceptibility to *F. tularensis* infection is in line with published data. This locus (termed the Bcg locus) harbors the *Slc11a1* gene encoding NRAMP1, which controls susceptibility to several intracellular bacteria, including *F. tularensis* (reviewed in reference 8). Sequenced genomes of B6 and AJ (from the Wellcome Trust Sanger database) show that AJ carries the Asp-169-Gly substitution, which was previously reported to confer sensitivity to *F. tularensis* infection (7), as well as a single nucleotide polymorphism (SNP) at the 3′ untranscribed region (UTR) of the *Slc11a1* gene. Although the variation at position 169 is known to affect susceptibility to *F. tularensis* infection, the SNP at the 3′ UTR has not been characterized. Our results not only confirm that natural variation in the NRAMP1 gene at the Bcg locus contributes to *F. tularensis* susceptibility but also suggest that two more previously unknown QTLs are present on chromosomes 2 and 19. The QTLs at the Bcg locus on chromosome 1 and the previously unpublished QTL on chromosome 2 seem to be interacting with each other; this interaction suggests that the genetic elements important in determining susceptibility to *F. tularensis* infection on these chromosomes are coregulated. The observation that the QTL on chromosome 19 found by *in vivo* analysis overlaps with that found by *in vitro* analysis suggests that a regulatory element may be shared in *in vitro* macrophage infection and *in vivo* intranasal infection.

TABLE 1 Upregulation of NFκB and IFN type I and II pathways in response to *F. tularensis* infection[a]

Mouse strain and cell type	2 h postinfection						10 h postinfection								
	NFκB canonical pathway			NFκB atypical pathway			Interferon signaling			Interferon α/β			Interferon γ		
	NES	Rank	*P* val	NES	Rank	*P* val	NES	Rank	*P* val	NES	Rank	*P* val	NES	Rank	*P* val
B6 Mø	2.075	6	<0.001	2.023	10	0.002	2.42	1	<0.001	2.34	2	<0.001	2.24	3	<0.001
AJ Mø	2.049	1	<0.001	1.97	6	0.002	2.12	2	<0.001	2.08	3	<0.001	2.07	4	<0.001

[a] NES, normalized enrichment score; Mø, macrophage; *P* val, *P* value.

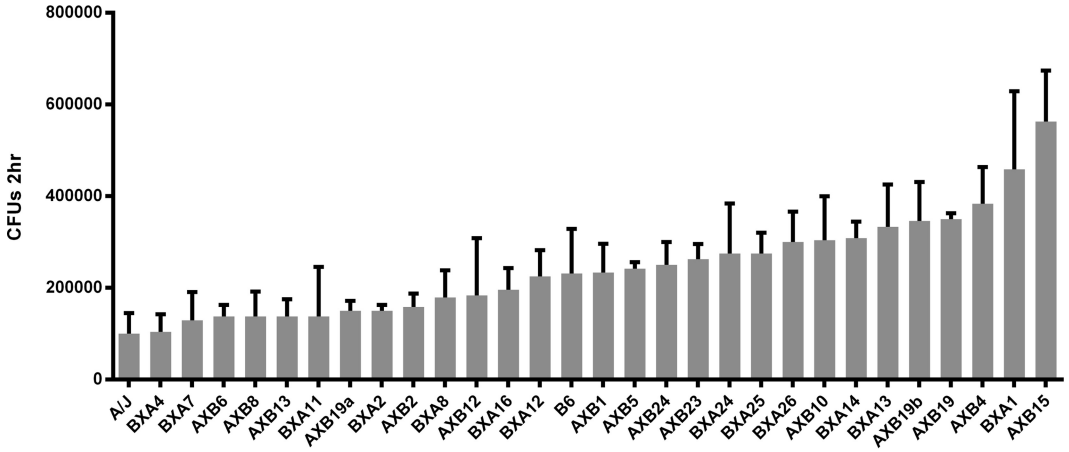

FIG 5 Intracellular bacterial numbers in the AJxB6 RI BMDM library 2 h after infection with *F. tularensis* LVS (MOI, 50). Strict measurement of only intracellular bacteria was performed (see Materials and Methods). Means and standard deviations are shown for each strain.

Although the chromosome 19 QTL is shared by the *in vitro* and *in vivo* infection models, it remains a daunting task to identify the exact genes within this region that control these phenotypic differences. The major obstacle is the fact that susceptibility to *F. tularensis* infection is a highly complex trait. As such, it involves the concerted interaction of many genes, with each individual gene making only a small contribution to the overall phenotype. This point is nicely illustrated by our observations in the *in vivo* infection model showing that all the QTLs found had similar LOD scores and that no QTL seemed to be more prominent than or dominant over the others. In addition, it has been suggested that the range of the genetic loci obtained from QTL analysis can cover ±10 to 20 cM (33), a value range that in this case corresponds to ~20 Mb and suggests many dozens of candidate genes. Often, the situation is made even more complicated by the interaction of several smaller QTLs within a larger QTL. In short, the situation is highly complex, potentially including the interaction of several individual genes (perhaps within the QTL) to produce the observed LOD signal. An examination of the literature indicates that few papers have described the exact gene within a QTL that is contributing to a given phenotype and that the great majority of QTL analyses have defined only the genetic loci associated with a specific phenotype (34, 35). Nevertheless, it is intriguing that early events during macrophage infection and bacterial counts during *in vivo* infection are associated with the same genetic locus. Further studies must better define the relationship between the *in vitro* and *in vivo* infection models and must determine whether early bacterium-macrophage associations *in vivo* can influence overall disease outcome.

Recent work has demonstrated that early interactions of *F. tularensis* with different macrophage surface molecules can affect the intracellular fate of the bacteria. Geier and Celli showed that association of complement-opsonized bacteria with CR3 prevents phagosome maturation and restricts phagosomal escape whereas association of IgG-opsonized bacteria with the Fc receptor enhances superoxide production and results in decreased intracellular proliferation (21). Furthermore, Dai et al. showed that interaction with CR3 inhibited TLR2 activation in an MKP1-dependent manner (29). Our work supports the idea that early events during *in vitro* bacterial infection influence the outcome of the infection. Higher bacterial counts at the initiation of infection are correlated with an altered transcriptional response and altered trafficking within macrophages. In addition, we propose for the first time that these kinetics of bacterial uptake and proliferation within the macrophage are influenced by the genetic background of the macrophages.

Enhanced transcription of several genes within the NFκB and IFN pathways in B6 BMDMs in response to *F. tularensis* infection is also intriguing. Among the genes that are upregulated in B6 macrophages in response to *F. tularensis* is that encoding IFN regulatory factor 1 (*Irf1*). This transcription factor was recently shown to be crucial for the activation of guanylate-binding proteins, ultimately promoting the killing of intracellular bacteria by these proteins (36). In addition, the fact that high TNF gene transcript levels were sustained in B6 but not in AJ macrophages in response to *F. tularensis* infection suggests a better response to *F. tularensis* infection in B6 BMDMs. Live *F. tularensis* can actively suppress TNF gene induction in a variety of human and mouse cells (37), whereas a mutant that is incapable of escaping the phagosome triggers constant activation and secretion of TNF-α. Similarly, active suppression of IFN-γ by *Francisella* results in improved bacterial survival inside mononuclear phagocytes (38). Taken together, these studies support the idea that the increased NFκB and IFN signaling by B6 is associated with the slower bacterial growth rate in these macrophages than in AJ macrophages. Further studies will explore whether this differential induction of major regulatory genes such as the *Irf1* gene and the *Tnf* gene occurs *in vivo* and what consequences of such differences are possible *in vivo*.

In summary, we have characterized some early interactions of macrophages with *F. tularensis* and have shown that these interactions are dependent on the host genetic background. In addition, we have identified novel QTLs associated with *in vitro* and *in vivo* susceptibility to *F. tularensis* infection. Our observation of the association of a specific genetic locus on chromosome 19 with both *in vitro* and *in vivo* infection models should facilitate further elucidation of the genetic circuits underlying differential susceptibilities to *F. tularensis* infection.

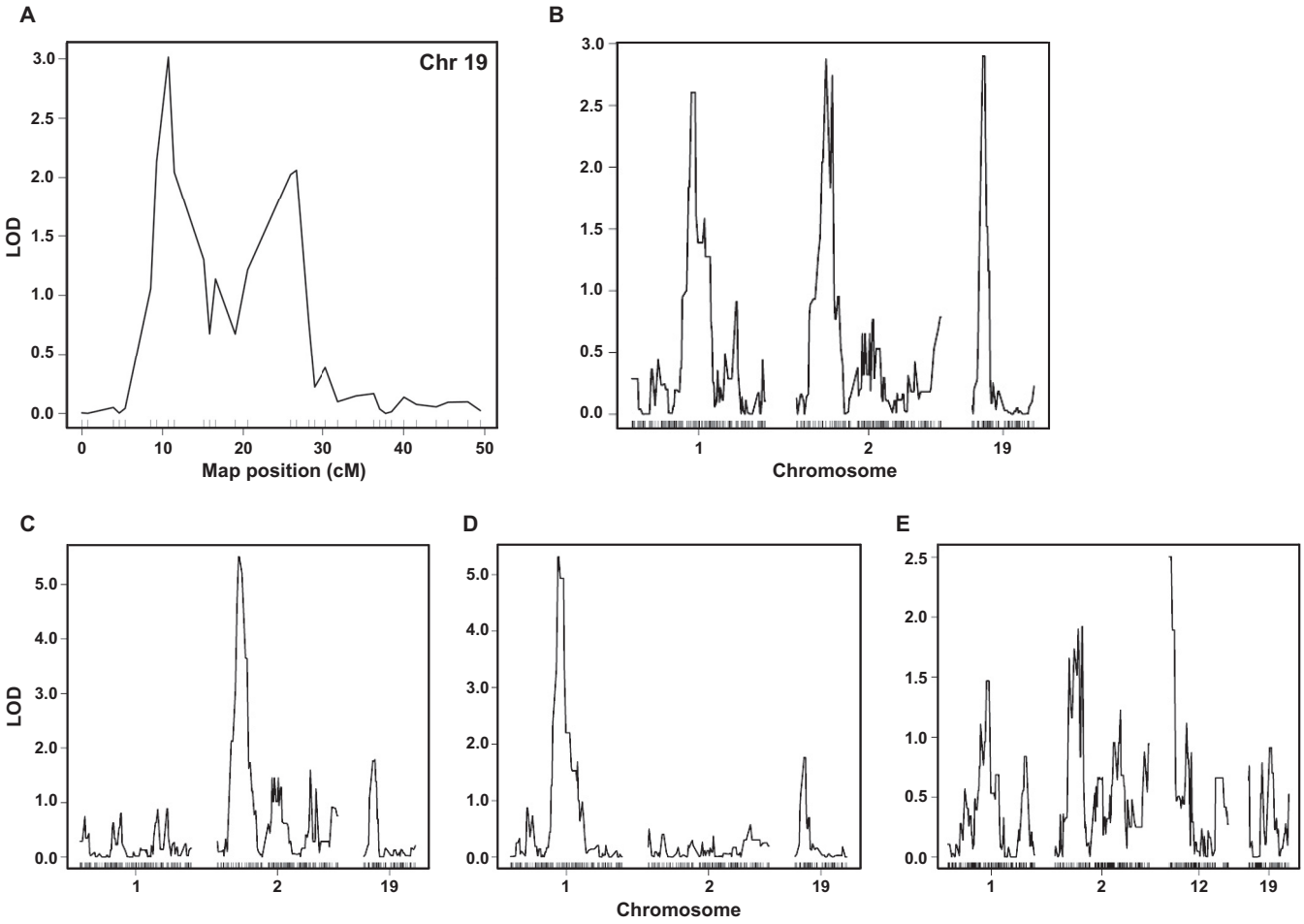

FIG 6 QTL analysis of *in vitro* and *in vivo* infection with *F. tularensis* LVS. (A) QTL analysis of bacterial counts 2 h after infection (see Fig. 5) revealed a locus on chromosome 19 (22.410 Mb) that was associated with this phenotype. (B) QTL analysis of LVS counts in spleen on day 5 after infection (see reference 5) showed three major loci on chromosomes 1 (79.900 Mb), 2 (27.662 Mb), and 19 (21.572 Mb), respectively. QTL positions on chromosome 19 are adjacent and overlapping. (C to E) *In vivo* QTL analysis showed that genetic loci on chromosomes 1 and 2 interact with each other, whereas the QTL on chromosome 19 does not interact with these loci. Fixing the genotype at the QTLs on chromosome 1 (C) and chromosome 2 (D) enhanced the signal for the QTLs on chromosomes 2 and 1, respectively. In contrast, fixing the genotype at the QTL on chromosome 19 (E) did not affect the QTLs on chromosomes 1 and 2.

MATERIALS AND METHODS

Ethics statement. Animal studies were carried out in strict accordance with the guidelines in the Guide for the Care and Use of Laboratory Animals (39). The protocol was approved by the Harvard Medical Area Standing Committee on Animals (protocol 04723) and the Massachusetts Institute of Technology Committee on Animal Care (assurance number A 3125-01; protocol number CAC 0611-063-14).

Bacterial strains and handling. *F. tularensis* LVS (kindly provided by Karen Elkins, U.S. Food and Drug Administration, Bethesda, MD) and fully virulent *F. tularensis* strain SchuS4 (provided by the Tufts New England Regional Biosafety Laboratory, Grafton, MA) were grown on cysteine heart agar plates supplemented with 1% hemoglobin (CHA) for 48 to 72 h at 37°C in 5% CO_2. For liquid medium cultures, bacteria were grown in tryptic soy broth (Difco, Detroit, MI) supplemented with ferric pyrophosphate and L-cysteine. *Salmonella enterica* serovar Typhimurium (SL1344) was grown on LB agar or broth supplemented with streptomycin sulfate (200 μg/ml).

***In vivo* experiments.** Male B6 or AJ specific-pathogen-free mice (Jackson Laboratory, Bar Harbor, ME) (6 to 8 weeks old) were housed in a biosafety level 2 (BL2) animal facility at Harvard Medical School. The mice, slightly anesthetized with isoflurane (Baxter, Deerfield, IL), were infected intranasally with 250 CFU of *F. tularensis* LVS in sterile phosphate-buffered saline (PBS) (50 μl) and followed for survival or bacterial burden.

To determine bacterial burden, mice were euthanized and specific tissues (lung, spleen, and liver) were collected 6 days after infection. Organs were weighed, hand-mashed, and homogenized with a Stomacher 80-paddle action blender (Seward, Port Saint Lucie, FL). Serial 10-fold dilutions were prepared with sterile PBS supplemented with 2% fetal bovine serum (FBS). A 10-μl volume of each dilution was plated onto CHA and incubated at 37°C in 5% CO_2 until colonies became visible (~48 h). Data were expressed as total CFU per organ.

Preparation of BMDMs and *in vitro* infection. Femurs of mice were collected and sterilized with 70% ethanol. Bone marrow was flushed with PBS, filtered, and spun down. The cell pellet was resuspended in supplemented BMDM growth medium—i.e., Dulbecco's modified Eagle's medium (DMEM) containing D-glucose (4.5 mg/liter), L-glutamine (4 mM), and sodium pyruvate (110 mg/liter) (Invitrogen, Carlsbad, CA) and supplemented with 10% heat-inactivated, low-endotoxin-unit FBS (Invitrogen) and 20% cell line L929-conditioned DMEM with nonessential amino acids. The cells from each femur were plated in 4 deep petri dishes, and the plates were incubated at 37°C in 5% CO_2. After 4 days, additional supplemented BMDM growth medium was added to petri dishes. Cells either were frozen on day 8 (FBS with 10% dimethyl sulfoxide [DMSO]) at

−180°C and kept for later use or were used directly for *in vitro* infection as described below.

On day 8, cells were detached from plates, counted, and plated (onto a 24-well plate at a density of 10^5 cells per well) in the presence of 10% L929-conditioned DMEM. The following day (day 9), bacteria (*F. tularensis* LVS or SchuS4) were streaked from a plate containing a 2- to 3-day-old culture and grown to an optical density (OD) of 0.3 (λ = 620 nm). Bacteria were spun and washed with sterile PBS (Invitrogen) and then resuspended in BMDM at an MOI of 50 or 100. Immediately before infection, cells were washed twice with PBS and the medium containing the bacteria was added. Cells were spun at 300 × *g* for 7 min to allow a synchronized infection starting point ($t = 0$). BMDMs and bacteria were incubated for 45 min and then washed twice, after which medium containing gentamicin (20 μg/ml) was added for 1 h. Cells were washed and either lysed with 1% saponin–PBS ($t = 2$ h) or supplemented with new medium and grown for an additional 22 h ($t = 24$ h) and lysed as described above. Bacteria in saponin were serially diluted in PBS and plated onto CHA. Growth was recorded 48 to 72 h later. This procedure is based on standard *in vitro* procedures described elsewhere (28, 40). Surplus cells that were not used for *in vitro* infection were frozen on day 8 (FBS with 10% DMSO) at −180°C and kept for later use. BMDMs from RI mice were obtained as described elsewhere (41).

FACS analysis. On day 8, BMDMs from AJ and B6 mice were detached from the plate with ice-cold PBS, spun down, and transferred to a round-bottom 96-well plate at a density of 2.5×10^5 to 5×10^5 cells per well. Cells were spun down at 500 × *g*, and PBS was replaced with 90 μl of fluorescence-activated cell sorter (FACS) buffer (10 mM EDTA, 15 mM sodium azide, 1% bovine serum albumin [BSA], PBS; pH 7.35) with a 1:100 concentration of Fc-blocking antibody (αCD16/32; BioLegend). Cells were incubated on ice for 30 min and then washed and incubated with antibodies to CD11b (BioLegend) and F4/80 (eBioscience) or isotype controls. After further incubation for 30 min, cells were washed and analyzed on a MACSQuant Analyzer (Miltenyi Biotec, San Diego, CA). Data were analyzed with FlowJo software (Ashland, OR).

Confocal microscopy. On day 6 or 7, BMDMs were counted and plated onto a 24-well plate containing a 1.5-thickness coverslip (Thermo Scientific) at a low density (5×10^4 cells per well). The following day, cells were washed and bacteria (*F. tularensis* LVS or *S.* Typhimurium) were added at an MOI of 50. Cells were centrifuged at 300 × *g* for 7 min to allow rapid bacterial adherence to cells, and slides were fixed (with 2.5% paraformaldehyde for 15 to 30 min and subsequent replacement with PBS) at 0, 10, 60, or 120 min after infection. Cells were permeabilized and blocked in PBS containing Triton X-100 (0.1%), horse serum (5%), and BSA (0.5%) for 30 min. Washing of cells with PBS was followed by the addition of the specific antibodies described for each experiment—i.e., antibodies to *F. tularensis* LPS (Abcam), *S.* Typhimurium LPS, EEA1, and LAMP1 (Santa Cruz). Incubation with primary antibody was followed by incubation with secondary antibody (Alexa Fluor; Invitrogen) and the specific fluorophores for 30 min. DAPI (4′,6-diamidino-2-phenylindole) (1 μg/ml) was added for 15 min. For actin staining, Alexa Fluor phalloidin (4 U/ml) was added for 20 min. Coverslips were washed, dried, and placed on the slide with 15 μl of mounting medium. Pictures were obtained with an Olympus FV1000 confocal microscope and were analyzed with Fiji software (42).

RNA sequencing (RNA-seq) and bioinformatic analysis. Frozen BMDMs were thawed and plated with supplemented DMEM as described above. On day 12, cells were counted and plated onto a 12-well plate at a density of 3×10^6 per well. The next day, cells were washed and bacteria (LVS) were added at an MOI of 100. Total RNA was extracted (RNeasy; Qiagen) at time zero (no bacteria) and at 2, 4, and 10 h after infection and was immediately stored at −80°C. Illumina library preparation, sequencing, and data processing were done as previously described (43). In brief, mRNA was purified from total RNA by poly(A)-tail enrichment (Dynabeads mRNA purification kit; Invitrogen), fragmented into 200 to 400 bp, and reverse transcribed into cDNA before Illumina sequencing adapters were added to each end. Libraries were barcoded, multiplexed into four samples per sequencing lane in the Illumina HiSeq 2000 system, and sequenced from both ends; this process resulted in 40-bp reads after the bar codes were discarded.

The RNA-seq reads were mapped to a synthetic mouse genome (mm10) in which all the single polymorphic nucleotides (as annotated by Wellcome Trust Sanger Institute sequencing; ftp://ftp-mouse.sanger.ac.uk/current_snps/) between AJ and B6 were masked with Bowtie2 (2.2.3) (44) and TopHat (v2.0.4) (45). Gene expression levels were then estimated as fragments per kilobase of exon per million fragments mapped (FPKM) in CuffLinks (v2.2.0) (46). At each time point, gene fold changes from baseline (defined as RNA levels from resting, uninfected, and unstimulated cells) were determined for both AJ and B6 BMDMs. The ranked lists of the fold changes (.rnk files) were analyzed by GSEA to determine which cellular pathways were upregulated, downregulated, or unchanged. With this platform, a total of 917 pathways were analyzed and scored. For samples from 2 and 10 h after infection, specific genes from each of the top 10 upregulated immunological pathways were combined and analyzed. Sorting and visualization of the data was done using SPIN (47). Genes with a 1.5-fold or greater difference between the AJ and B6 results were plotted.

QTL mapping. The genomic loci that regulate bacterial burden in AXB/BXA BMDMs were determined as previously described (43). In brief, we used 934 AXB/BXA genetic informative markers obtained from http://www.genenetwork.org to perform a genome-wide scan in R/qtl (48). The significance of QTL LOD scores was assessed with 1,000 permutations of the phenotype data, as has been described (49), and the corresponding *P* values were reported. QTL significance was reported at a genome-wide threshold corresponding to *P* values of <0.05.

SUPPLEMENTAL MATERIAL

Supplemental material for this article may be found at http://mbio.asm.org/lookup/suppl/doi:10.1128/mBio.02243-15/-/DCSupplemental.

Figure S1, TIF file, 0.04 MB.
Figure S2, TIF file, 0.02 MB.
Figure S3, TIF file, 0.2 MB.

ACKNOWLEDGMENTS

We are grateful to Rebecca A. Betensky (Harvard School of Public Health) for her help with the statistical analysis. We thank the Tufts New England Regional Biosafety Laboratory (RBL) team for their contribution to the ShuS4 studies. We are also grateful to Jerry Beltz and Neeraj K. Surana for fruitful discussions and to Ria Roberts, Alec Derian, and Bella Printseva (Harvard Medical School, Boston) for their technical assistance.

This study was supported by the New England Center of Excellence in Biodefense and Emerging Infectious Diseases under grant AI057159 from the National Institute of Allergy and Infectious Diseases. The funders had no role in study design, data collection and analysis, decision to publish, or preparation of the manuscript.

FUNDING INFORMATION

This work, including the efforts of Avner Fink, Musa A. Hassan, Nihal A. Okan, Michal Sheffer, Ana Camejo, Jeroen P.J. Saeij, and Dennis L. Kasper, was funded by HHS | NIH | National Institute of Allergy and Infectious Diseases (NIAID) (AI057159).

Wellcome Trust-Massachusetts Institute of Technology (http://www.wellcome.ac.uk) Postdoctoralt Fellowship and Recruitment Enhancement was awarded to Musa A. Hassan.

The funders had no role in study design, data collection and analysis, decision to publish, or preparation of the manuscript.

REFERENCES

1. **Bosio CM, Dow SW.** 2005. Francisella tularensis induces aberrant activation of pulmonary dendritic cells. J Immunol 175:6792–6801. http://dx.doi.org/10.4049/jimmunol.175.10.6792.

2. **Elkins KL, Rhinehart-Jones TR, Culkin SJ, Yee D, Winegar RK.** 1996. Minimal requirements for murine resistance to infection with Francisella tularensis LVS. Infect Immun **64:**3288–3293.
3. **Roberts LM, Tuladhar S, Steele SP, Riebe KJ, Chen CJ, Cumming RI, Seay S, Frothingham R, Sempowski GD, Kawula TH, Frelinger JA.** 2014. Identification of early interactions between Francisella and the host. Infect Immun **82:**2504–2510. http://dx.doi.org/10.1128/IAI.01654-13.
4. **Sebastian S, Pinkham JT, Lynch JG, Ross RA, Reinap B, Blalock LT, Conlan JW, Kasper DL.** 2009. Cellular and humoral immunity are synergistic in protection against types A and B Francisella tularensis. Vaccine **27:**597–605. http://dx.doi.org/10.1016/j.vaccine.2008.10.079.
5. **Anthony LS, Skamene E, Kongshavn PA.** 1988. Influence of genetic background on host resistance to experimental murine tularemia. Infect Immun **56:**2089–2093.
6. **Fortier AH, Slayter MV, Ziemba R, Meltzer MS, Nacy CA.** 1991. Live vaccine strain of Francisella tularensis: infection and immunity in mice. Infect Immun **59:**2922–2928.
7. **Kovárová H, Hernychová L, Hajdúch M, Sírová M, Macela A.** 2000. Influence of the bcg locus on natural resistance to primary infection with the facultative intracellular bacterium Francisella tularensis in mice. Infect Immun **68:**1480–1484. http://dx.doi.org/10.1128/IAI.68.3.1480-1484.2000.
8. **Fortier A, Min-Oo G, Forbes J, Lam-Yuk-Tseung S, Gros P.** 2005. Single gene effects in mouse models of host:pathogen interactions. J Leukoc Biol **77:**868–877.
9. **Kovárová H, Halada P, Man P, Golovliov I, Krocová Z, Spacek J, Porkertová S, Necasová R.** 2002. Proteome study of Francisella tularensis live vaccine strain-containing phagosome in Bcg/Nramp1 congenic macrophages: resistant allele contributes to permissive environment and susceptibility to infection. Proteomics **2:**85–93. http://dx.doi.org/10.1002/1615-9861(200201)2:1<85::AID-PROT85>3.0.CO;2-S.
10. **Andersson H, Hartmanová B, Kuolee R, Rydén P, Conlan W, Chen W, Sjöstedt A.** 2006. Transcriptional profiling of host responses in mouse lungs following aerosol infection with type A Francisella tularensis. J Med Microbiol **55:**263–271. http://dx.doi.org/10.1099/jmm.0.46313-0.
11. **Anthony LS, Ghadirian E, Nestel FP, Kongshavn PA.** 1989. The requirement for gamma interferon in resistance of mice to experimental tularemia. Microb Pathog **7:**421–428.
12. **Malik M, Bakshi CS, Sahay B, Shah A, Lotz SA, Sellati TJ.** 2006. Toll-like receptor 2 is required for control of pulmonary infection with Francisella tularensis. Infect Immun **74:**3657–3662. http://dx.doi.org/10.1128/IAI.02030-05.
13. **Rathinam VA, Jiang Z, Waggoner SN, Sharma S, Cole LE, Waggoner L, Vanaja SK, Monks BG, Ganesan S, Latz E, Hornung V, Vogel SN, Szomolanyi-Tsuda E, Fitzgerald KA.** 2010. The AIM2 inflammasome is essential for host defense against cytosolic bacteria and DNA viruses. Nat Immunol **11:**395–402. http://dx.doi.org/10.1038/ni.1864.
14. **Storek KM, Gertsvolf NA, Ohlson MB, Monack DM.** 2015. cGAS and Ifi204 cooperate to produce type I IFNs in response to Francisella infection. J Immunol **194:**3236–3245. http://dx.doi.org/10.4049/jimmunol.1402764.
15. **Jones CL, Sampson TR, Nakaya HI, Pulendran B, Weiss DS.** 2012. Repression of bacterial lipoprotein production by Francisella novicida facilitates evasion of innate immune recognition. Cell Microbiol **14:**1531–1543. http://dx.doi.org/10.1111/j.1462-5822.2012.01816.x.
16. **Thakran S, Li H, Lavine CL, Miller MA, Bina JE, Bina XR, Re F.** 2008. Identification of Francisella tularensis lipoproteins that stimulate the Toll-like receptor (TLR) 2/TLR1 heterodimer. J Biol Chem **283:**3751–3760. http://dx.doi.org/10.1074/jbc.M706854200.
17. **Bauler TJ, Chase JC, Bosio CM.** 2011. IFN-beta mediates suppression of IL-12p40 in human dendritic cells following infection with virulent Francisella tularensis. J Immunol **187:**1845–1855. http://dx.doi.org/10.4049/jimmunol.1100377.
18. **Dotson RJ, Rabadi SM, Westcott EL, Bradley S, Catlett SV, Banik S, Harton JA, Bakshi CS, Malik M.** 2013. Repression of inflammasome by Francisella tularensis during early stages of infection. J Biol Chem **288:**23844–23857. http://dx.doi.org/10.1074/jbc.M113.490086.
19. **Jones CL, Napier BA, Sampson TR, Llewellyn AC, Schroeder MR, Weiss DS.** 2012. Subversion of host recognition and defense systems by Francisella spp. Microbiol Mol Biol Rev **76:**383–404. http://dx.doi.org/10.1128/MMBR.05027-11.
20. **Sjöstedt A.** 2007. Tularemia: history, epidemiology, pathogen physiology, and clinical manifestations. Ann N Y Acad Sci **1105:**1–29. http://dx.doi.org/10.1196/annals.1409.009.
21. **Geier H, Celli J.** 2011. Phagocytic receptors dictate phagosomal escape and intracellular proliferation of Francisella tularensis. Infect Immun **79:**2204–2214. http://dx.doi.org/10.1128/IAI.01382-10.
22. **Pierini LM.** 2006. Uptake of serum-opsonized Francisella tularensis by macrophages can be mediated by class A scavenger receptors. Cell Microbiol **8:**1361–1370. http://dx.doi.org/10.1111/j.1462-5822.2006.00719.x.
23. **Balagopal A, MacFarlane AS, Mohapatra N, Soni S, Gunn JS, Schlesinger LS.** 2006. Characterization of the receptor-ligand pathways important for entry and survival of Francisella tularensis in human macrophages. Infect Immun **74:**5114–5125. http://dx.doi.org/10.1128/IAI.00795-06.
24. **Schulert GS, Allen LA.** 2006. Differential infection of mononuclear phagocytes by Francisella tularensis: role of the macrophage mannose receptor. J Leukoc Biol **80:**563–571. http://dx.doi.org/10.1189/jlb.0306219.
25. **Asare R, Kwaik YA.** 2010. Exploitation of host cell biology and evasion of immunity by Francisella tularensis. Front Microbiol **1:**145. http://dx.doi.org/10.3389/fmicb.2010.00145.
26. **Nesbitt MN, Skamene E.** 1984. Recombinant inbred mouse strains derived from A/J and C57BL/6J: a tool for the study of genetic mechanisms in host resistance to infection and malignancy. J Leukoc Biol **36:**357–364.
27. **Hassan MA, Jensen KD, Butty V, Hu K, Boedec E, Prins P, Saeij JP.** 2015. Transcriptional and linkage analyses identify loci that mediate the differential macrophage response to inflammatory stimuli and infection. PLoS Genet **11:**e1005619. http://dx.doi.org/10.1371/journal.pgen.1005619.
28. **Platz GJ, Bublitz DC, Mena P, Benach JL, Furie MB, Thanassi DG.** 2010. A tolC mutant of Francisella tularensis is hypercytotoxic compared to the wild type and elicits increased proinflammatory responses from host cells. Infect Immun **78:**1022–1031. http://dx.doi.org/10.1128/IAI.00992-09.
29. **Dai S, Rajaram MV, Curry HM, Leander R, Schlesinger LS.** 2013. Fine tuning inflammation at the front door: macrophage complement receptor 3-mediates phagocytosis and immune suppression for Francisella tularensis. PLoS Pathog **9:**e1003114. http://dx.doi.org/10.1371/journal.ppat.1003114.
30. **Peng K, Broz P, Jones J, Joubert LM, Monack D.** 2011. Elevated AIM2-mediated pyroptosis triggered by hypercytotoxic Francisella mutant strains is attributed to increased intracellular bacteriolysis. Cell Microbiol **13:**1586–1600. http://dx.doi.org/10.1111/j.1462-5822.2011.01643.x.
31. **Abiola O, Angel JM, Avner P, Bachmanov AA, Belknap JK, Bennett B, Blankenhorn EP, Blizard DA, Bolivar V, Brockmann GA, Buck KJ, Bureau JF, Casley WL, Chesler EJ, Cheverud JM, Churchill GA, Cook M, Crabbe JC, Crusio WE, Darvasi A, de Haan G, Dermant P, Doerge RW, Elliot RW, Farber CR, Flaherty L, Flint J, Gershenfeld H, Gibson JP, Gu J, Gu W, Himmelbauer H, Hitzemann R, Hsu HC, Hunter K, Iraqi FF, Jansen RC, Johnson TE, Jones BC, Kempermann G, Lammert F, Lu L, Manly KF, Matthews DB, Medrano JF, Mehrabian M, Mittlemann G, Mock BA, Mogil JS, Montagutelli X, et al.** 2003. The nature and identification of quantitative trait loci: a community's view. Nat Rev Genet **4:**911–916. http://dx.doi.org/10.1038/nrg1206.
32. **Cox RD, Brown SD.** 2003. Rodent models of genetic disease. Curr Opin Genet Dev **13:**278–283. http://dx.doi.org/10.1016/S0959-437X(03)00051-0.
33. **Holland JB.** 2007. Genetic architecture of complex traits in plants. Curr Opin Plant Biol **10:**156–161. http://dx.doi.org/10.1016/j.pbi.2007.01.003.
34. **Ermann J, Glimcher LH.** 2012. After GWAS: mice to the rescue? Curr Opin Immunol **24:**564–570. http://dx.doi.org/10.1016/j.coi.2012.09.005.
35. **Roff DA.** 2007. A centennial celebration for quantitative genetics. Evolution **61:**1017–1032. http://dx.doi.org/10.1111/j.1558-5646.2007.00100.x.
36. **Man SM, Karki R, Malireddi RK, Neale G, Vogel P, Yamamoto M, Lamkanfi M, Kanneganti TD.** 2015. The transcription factor IRF1 and guanylate-binding proteins target activation of the AIM2 inflammasome by Francisella infection. Nat Immunol **16:**467–475. http://dx.doi.org/10.1038/ni.3118.
37. **Telepnev M, Golovliov I, Sjöstedt A.** 2005. Francisella tularensis LVS initially activates but subsequently down-regulates intracellular signaling and cytokine secretion in mouse monocytic and human peripheral blood mononuclear cells. Microb Pathog **38:**239–247. http://dx.doi.org/10.1016/j.micpath.2005.02.003.
38. **Parsa KV, Butchar JP, Rajaram MV, Cremer TJ, Gunn JS, Schlesinger LS, Tridandapani S.** 2008. Francisella gains a survival advantage within mononuclear phagocytes by suppressing the host

IFNgamma response. Mol Immunol **45:**3428–3437. http://dx.doi.org/10.1016/j.molimm.2008.04.006.

39. **National Research Council (U.S.), Committee for the Update of the Guide for the Care and Use of Laboratory Animals, Institute for Laboratory Animal Research (U.S.), National Academies Press (U.S.).** 2011. Guide for the Care and Use of Laboratory Animals, 8th ed. National Academies Press, Washington, DC.
40. **Okan NA, Chalabaev S, Kim TH, Fink A, Ross RA, Kasper DL.** 2013. Kdo hydrolase is required for Francisella tularensis virulence and evasion of TLR2-mediated innate immunity. mBio **4:**e00638-12. http://dx.doi.org/10.1128/mBio.00638-12.
41. **Jensen KD, Wang Y, Wojno ED, Shastri AJ, Hu K, Cornel L, Boedec E, Ong Y-C, Chien YH, Hunter CA, Boothroyd JC, Saeij JP.** 2011. Toxoplasma polymorphic effectors determine macrophage polarization and intestinal inflammation. Cell Host Microbe **9:**472–483. http://dx.doi.org/10.1016/j.chom.2011.04.015.
42. **Schindelin J, Arganda-Carreras I, Frise E, Kaynig V, Longair M, Pietzsch T, Preibisch S, Rueden C, Saalfeld S, Schmid B, Tinevez JY, White DJ, Hartenstein V, Eliceiri K, Tomancak P, Cardona A.** 2012. Fiji: an open-source platform for biological-image analysis. Nat Methods **9:**676–682. http://dx.doi.org/10.1038/nmeth.2019.
43. **Hassan MA, Butty V, Jensen KD, Saeij JP.** 2014. The genetic basis for individual differences in mRNA splicing and APOBEC1 editing activity in murine macrophages. Genome Res **24:**377–389. http://dx.doi.org/10.1101/gr.166033.113.
44. **Langmead B, Trapnell C, Pop M, Salzberg SL.** 2009. Ultrafast and memory-efficient alignment of short DNA sequences to the human genome. Genome Biol **10:**R25. http://dx.doi.org/10.1186/gb-2009-10-3-r25.
45. **Trapnell C, Pachter L, Salzberg SL.** 2009. TopHat: discovering splice junctions with RNA-Seq. Bioinformatics **25**(9):1105–1111. http://dx.doi.org/10.1093/bioinformatics/btp120.
46. **Trapnell C, Hendrickson DG, Sauvageau M, Goff L, Rinn JL, Pachter L.** 2013. Differential analysis of gene regulation at transcript resolution with RNA-seq. Nat Biotechnol **31:**46–53. http://dx.doi.org/10.1038/nbt.2450.
47. **Tsafrir D, Tsafrir I, Ein-Dor L, Zuk O, Notterman DA, Domany E.** 2005. Sorting points into neighborhoods (SPIN): data analysis and visualization by ordering distance matrices. Bioinformatics **21:**2301–2308.
48. **Broman KW, Wu H, Sen S, Churchill GA.** 2003. R/qtl: QTL mapping in experimental crosses. BioInformatics **19:**889–890. http://dx.doi.org/10.1093/bioinformatics/btg112.
49. **Churchill GA, Doerge RW.** 1994. Empirical threshold values for quantitative trait mapping. Genetics **138:**963–971.